Analysis and Design of Full-Bridge Class-DE Inverter at Fixed Duty Cycle

Luca Albertoni, Francesco Grasso, Jacopo Matteucci,
Maria C. Piccirilli, Alberto Reatti
DINFO-University of Florence
Via Santa Marta 3 I-50139 Florence
{luca.albertoni, jacopo.matteucci}@stud.unifi.it
{francesco.grasso, mariacristina.piccirilli, alberto.reatti}@unifi.it

Agasthya Ayachit, Marian K. Kazimierczuk
Department of Electrical Engineering
Wright State University
3640 Colonel Glenn Hwy.,
Dayton, OH, 45435, USA
{ayachit.2, marian.kazimierczuk}@wright.edu

***Abstract*—This paper presents the following for a full-bridge Class-DE resonant inverter operating at a fixed duty ratio: (a) steady-state analysis using first-harmonic approximation and (b) derivation of closed-form expressions for the currents, voltages, and powers. The conversion from a series-parallel resonant network to a series resonant network is presented. Imposing the zero-voltage and zero-derivative switching conditions, the expression for a shunt capacitance across the MOSFETs in the inverter bridge is derived. The closed-form expressions to calculate the values of the resonant components are presented. A practical design of a Class-DE resonant inverter supplied by a dc input voltage of 230 V, delivering an output power of 920 W, and operating at a switching frequency of 100 kHz is considered and its design methodology is included. Theoretical results are validated by Saber simulations.**

I. Introduction

Class-DE inverters are a family of power electronic topologies for energy conversion, which are duly characterized by high efficiency [1]-[4]. An interesting feature of the Class-DE topology is their ability to achieve both zero-voltage switching (ZVS) and zero-derivative switching (ZDS) conditions, thereby yielding high power-conversion efficiency, especially at high switching frequencies. This makes them suitable for applications such as RF power supplies and RF power amplifiers [3], induction heating [4], on-chip converters [5], [6], wireless-power transfer systems [7], [8], [20], etc. The Class-DE inverter shares a few features of Class-E as well as Class-D inverters making them an ideal choice for high-power applications [8], [12]-[19].

Several works in the literature related to the Class-DE inverter have focused on the following areas: steady-state analysis with half-bridge switching network at a fixed and any duty ratio [1], [5], [9], [12] and design of inverter with with linear and nonlinear shunt MOSFET capacitances [2], [14], [16], [17]. However, a detailed steady-state analysis of a full-bridge Class-DE inverter at any duty cycle has not been reported. Therefore, this paper aims at the following objectives: (a) develop a theoretical framework for the steady-state characteristics of the full-bridge Class-DE inverter operating at any duty ratio using the fundamental harmonic approximation, (b) derive the expressions for the shunt capacitances and the components in the resonant circuit, (c) develop a methodology to transform a series-parallel topology of the inverter to its series resonant form and *vice versa*, and (d) analyze its voltage transfer function, input impedance, and efficiency. A high-power, high-frequency full-bridge Class-DE inverter is designed. Saber circuit simulations are provided to validate the correctness of the theoretically analysis. The switching-network waveforms demonstrate ZVS operation, while an efficiency of 97% is achieved.

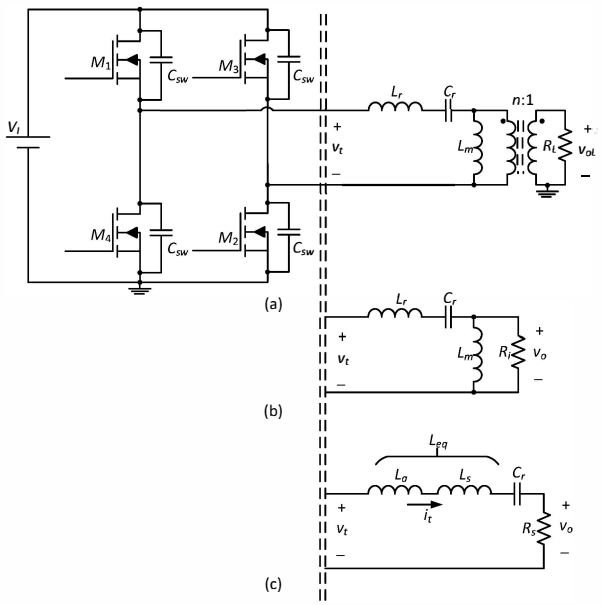

Fig. 1. Circuits of the full-bridge class-DE resonant inverter. (a) Series-parallel resonant circuit with transformer. (b) Series-parallel resonant circuit with load resistance on primary side. (c) Series resonant circuit.

II. Full-Bridge Class-DE DC-AC Inverter Analysis

A. Circuit Description

Fig. 1(a) shows the circuit of the full-bridge Class-DE series resonant inverter with a transformer. The circuit constitutes four MOSFETs each of them with a shunt capacitor C_{sw}, which are used to minimize the switching losses of these devices. The inverter is supplied by a DC voltage V_I and

978-1-5090-3474-1/16/$31.00 ©2016 IEEE

feeds a resonant tank circuit with a square-wave voltage. The switching frequency is f_s. The anti-parallel diodes provides a path for the current to flow from the source to the drain during the instants, when the switches are OFF. The pulse-width of the gate signal has a duty cycle D. Each MOSFET remains ON for an interval DT, where $T = 1/f_s$ is the switching time period. The gate signals to the switches M_1 and M_4 are 180° out of phase with those provided to the switches M_2 and M_3. The duty cycle chosen for each switch is lower than 0.5, thereby providing a finite dead time between the switching instants. The shunt capacitors in parallel with the MOSFETs are used to shape the voltage across the MOSFETs in order to achieve ZVS condition under certain operating conditions.

In Fig. 1(a), the series resonant circuit consists of a resonant capacitor C_r and a resonant inductor L_a, while L_m represents the magnetizing inductance of the transformer. Fig. 1(b) illustrates the use of reflection principle to transfer the load resistance R_L to the primary side forming the series-parallel resonant network. Fig. 1(c) shows the conversion of the series-parallel network comprising of $L_r - C_r - L_m - R_i$ to a series resonant network comprising of $L_a - C_r - L_s - R_s$. Due to a high quality factor of these components, only the first harmonic of the tank voltage and current is delivered to the load.

B. Circuit Analysis

Analysis of a series resonant network is by far easier than the series-parallel topology. Therefore, a comprehensive analysis of the inverter is first performed on the series resonant circuit. Then, using appropriate transformation principles, the series topology shown in Fig. 1(a) is converted to series-parallel topology shown in Fig. 1(b). The first harmonic approximation is used to determine the inverter currents and voltages [12]. The subsequent analysis of the inverter is based on the following assumptions:

1) The converter operates in steady state.
2) The current through the resonant tank is purely sinusoidal.
3) The circuit components are assumed to be ideal and all the parasitic components are neglected.
4) The DC supply voltage and the amplitude of the output voltage are constant.
5) Only the fundamental component is responsible for delivering the rated power to the load resistance.

The steady-state expressions and design equations consider a duty cycle of $D = 0.4$. Therefore, each MOSFET is ON for $4\pi/5$. A symmetrical dead time of $t_d = \pi/5$ is chosen at the beginning of each turn-ON event. The current through the resonant tank is

$$i_{tan} = I_m \sin(\omega t + \phi), \tag{1}$$

where I_m is the amplitude of the sinusoidal current waveform, $\omega = 2\pi f_s$ is the angular operating frequency with $0 < \omega t \leq 2\pi$ and ϕ is the phase shift between the tank current and the tank voltage. Each switching period is divided into four time intervals as shown in Table I. Fig. 2 shows the key current and

TABLE I
TIME INTERVAL AND STATE OF THE MOSFETS AT $D = 0.4$.

Interval	Time	State
t_A=$[t_1, t_2]$	$\pi/10 \leq \omega t < 9\pi/10$	$M_{1,2}$ on, $M_{3,4}$ off
t_B=$[t_2, t_3]$	$9\pi/10 \leq \omega t < 11\pi/10$	$M_{1,2,3,4}$ off
t_C=$[t_3, t_4]$	$11\pi/10 \leq \omega t < 19\pi/10$	$M_{1,2}$ on, $M_{3,4}$ off
t_D=$[t_4, t_1]$	$19\pi/10 \leq \omega t < 21\pi/10$	$M_{1,2,3,4}$ off

voltage waveforms during indicating the state of the inverter during each sub-interval. During time interval t_A, M_1 and M_2 are ON to give

$$\begin{aligned} v_{DS1} &= v_{DS2} = 0 \\ v_{DS3} &= v_{DS4} = V_I. \end{aligned} \tag{2}$$

Since the voltage across the shunt capacitances are constant, their currents are equal to zero. During the interval t_B, the capacitors C_{sw1} and C_{sw2} begin to charge, while the capacitors C_{sw3} and C_{sw4} begin to discharge. Applying the KVL and KCL to the nodes and the meshes of the circuit, we obtain the following equations.

$$V_I = v_{DS1} + v_{DS4} = v_{DS3} + v_{DS2}, \tag{3}$$

$$i_{tan} = i_{CSW1} - i_{CSW4} = i_{CSW2} - i_{CSW3}. \tag{4}$$

Combination of (3) and (4) and their derivative results in

$$\begin{cases} i_{tan} = \omega C_{sw1} \frac{dv_{DS1}}{d(\omega t)} - \omega C_{sw4} \frac{dv_{DS4}}{d(\omega t)} \\ i_{tan} = \omega C_{sw2} \frac{dv_{DS2}}{d(\omega t)} - \omega C_{sw3} \frac{dv_{DS3}}{d(\omega t)} \end{cases} \tag{5}$$

where

$$\begin{cases} \frac{dv_{DS1}}{d(\omega t)} = -\frac{dv_{DS4}}{d(\omega t)} = \frac{I_m}{\omega(C_{sw1}+C_{sw4})} \sin(\omega t + \phi) \\ \frac{dv_{DS2}}{d(\omega t)} = -\frac{dv_{DS3}}{d(\omega t)} = \frac{I_m}{\omega(C_{sw2}+C_{sw3})} \sin(\omega t + \phi.) \end{cases} \tag{6}$$

Imposing zero-derivative switching (ZDS) for the voltages across the MOSFETs, during turn ON at $\omega t = \pi/10$, we get

$$\sin\left(\frac{\pi}{10} + \phi\right) = 0 \tag{7}$$

to yield

$$\phi = -\frac{\pi}{10}. \tag{8}$$

Thus, solving for capacitor currents provide

$$\begin{cases} i_{Csw1} = \frac{C_{sw1}}{(C_{sw1}+C_{sw4})} I_m \sin\left(\omega t - \frac{\pi}{10}\right) \\ i_{Csw2} = \frac{C_{sw2}}{(C_{sw2}+C_{sw3})} I_m \sin\left(\omega t - \frac{\pi}{10}\right) \\ i_{Csw3} = -\frac{C_{sw3}}{(C_{sw2}+C_{sw3})} I_m \sin\left(\omega t - \frac{\pi}{10}\right) \\ i_{Csw4} = -\frac{C_{sw4}}{(C_{sw1}+C_{sw4})} I_m \sin\left(\omega t - \frac{\pi}{10}\right) \end{cases} \tag{9}$$

and solving for the switch voltages yields

$$\begin{cases} v_{DS1} = \frac{I_m}{\omega(C_{sw1}+C_{sw4})} \left[-\cos\left(\omega t + \frac{\pi}{10}\right) + \cos\left(\frac{\pi}{5}\right)\right] \\ v_{DS2} = \frac{I_m}{\omega(C_{sw2}+C_{sw3})} \left[-\cos\left(\omega t + \frac{\pi}{10}\right) + \cos\left(\frac{\pi}{5}\right)\right] \\ v_{DS3} = \frac{I_m}{\omega(C_{sw2}+C_{sw3})} \left[-\cos\left(\omega t + \frac{\pi}{10}\right) + \cos\left(\frac{\pi}{5}\right)\right] + V_I \\ v_{DS4} = \frac{I_m}{\omega(C_{sw1}+C_{sw4})} \left[-\cos\left(\omega t + \frac{\pi}{10}\right) + \cos\left(\frac{\pi}{5}\right)\right] + V_I. \end{cases} \tag{10}$$

Imposing the zero-voltage switching (ZVS) condition to v_{DS3}

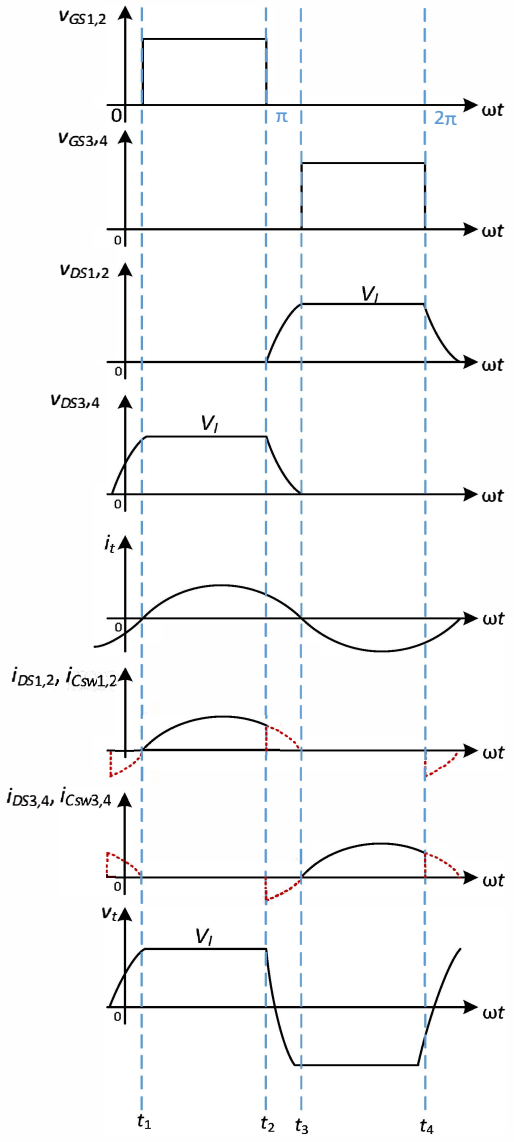

Fig. 2. Waveforms of switch currents, switch voltages, capacitor current, resonant current, and the resonant tank voltage.

and v_{DS4} at the end of time interval t_B at $\omega t = 11\pi/10$, we get

$$C_{sw1} + C_{sw4} = C_{sw2} + C_{sw3}, \tag{11}$$

to give

$$I_m = \frac{C_{sw1} + C_{sw4}}{1 - \cos\frac{\pi}{5}}\omega V_I = 5.236\left(C_{sw1} + C_{sw4}\right)\omega V_I. \tag{12}$$

During time interval t_C, M_3 and M_4 are ON. Therefore,

$$\begin{aligned} v_{DS1} &= v_{DS2} = V_I \\ v_{DS3} &= v_{DS4} = 0. \end{aligned} \tag{13}$$

Finally, during the interval t_D, the circuit configuration is dual with respect to that achieved during time interval t_B, where the currents and voltage are displaced exactly by 180°. The current and voltage expressions are

$$\begin{aligned} i_{Csw1} &= \tfrac{C_{sw1}}{(C_{sw1}+C_{sw4})} I_m \sin\left(\omega t - \tfrac{\pi}{10}\right) \\ i_{Csw2} &= \tfrac{C_{sw2}}{(C_{sw2}+C_{sw3})} I_m \sin\left(\omega t - \tfrac{\pi}{10}\right) \\ i_{Csw3} &= -\tfrac{C_{sw3}}{(C_{sw2}+C_{sw3})} I_m \sin\left(\omega t - \tfrac{\pi}{10}\right) \\ i_{Csw4} &= -\tfrac{C_{sw4}}{(C_{sw1}+C_{sw4})} I_m \sin\left(\omega t - \tfrac{\pi}{10}\right). \end{aligned} \tag{14}$$

and

$$\begin{cases} v_{DS1} = \frac{I_m}{\omega(C_{sw1}+C_{sw4})}\left[\cos\left(\omega t + \frac{\pi}{10}\right) - \cos\left(\frac{\pi}{5}\right)\right] \\ v_{DS2} = \frac{I_m}{\omega(C_{sw2}+C_{sw3})}\left[+\cos\left(\omega t + \frac{\pi}{10}\right) - \cos\left(\frac{\pi}{5}\right)\right] \\ v_{DS3} = \frac{I_m}{\omega(C_{sw2}+C_{sw3})}\left[-\cos\left(\omega t + \frac{\pi}{10}\right) + \cos\left(\frac{\pi}{5}\right)\right] + V_I \\ v_{DS4} = \frac{I_m}{\omega(C_{sw1}+C_{sw4})}\left[-\cos\left(\omega t + \frac{\pi}{10}\right) + \cos\left(\frac{\pi}{5}\right)\right] + V_I. \end{cases} \tag{15}$$

III. Closed-Form Expressions

A. Currents, Voltages, and Powers

The average dc input current can be determined as follows. During t_A between $\frac{\pi}{10} < \omega t \leq \frac{9\pi}{10}$, $i_{tan} = i_{DS1}$. Similarly, during t_C between $\frac{11\pi}{10} < \omega t \leq \frac{19\pi}{10}$, $i_{tan} = i_{DS2}$. By considering the overall tank current using (5), we obtain the average dc input current as

$$I_I = \frac{1}{2\pi}\int_0^{2\pi} i_{tan} d\left(\omega t\right) = \frac{I_m}{2\pi}. \tag{16}$$

Similarly, the tank voltage applied to the resonant circuit is

$$v_{tan} = v_{DS3} - v_{DS1}. \tag{17}$$

A Fourier series expansion of v_{tan} given in (17) yields

$$v_{tan} = \frac{1}{2}a_0 + \sum_{n=1}^{\infty} a_n \cos\left(n\omega t - \phi\right) + b_n \sin\left(n\omega t - \phi\right). \tag{18}$$

In (18), $a_0 = 0$, since v_{tan} has odd symmetry. From Fig. 1, at resonance, the voltage drops across C_r and L_a are equal and out of phase by 180° canceling out each other. Thus, for the fundamental component ($n = 1$) and the applied tank voltage becomes

$$v_{tan} = v_{Ls} + v_o = V_{Lm}\cos\left(\omega t - \frac{\pi}{10}\right) + V_m \sin\left(\omega t - \frac{\pi}{10}\right). \tag{19}$$

The Fourier coefficients are $a_n = V_{Lm}$ and $b_n = V_m$, whose expressions are determined as follows. From the principle of Fourier series, the amplitude of the voltage across the inductance L_s is defined as

$$\begin{aligned} V_{Lm} &= \frac{1}{\pi}\int_0^{2\pi}\left(v_{DS3} - v_{DS1}\right)\cos\left(\omega t + \frac{9\pi}{10}\right) d\left(\omega t\right) \\ &= V_I \frac{\sin\frac{8\pi}{5} + \frac{2\pi}{5}}{\pi\left(1 + \cos\frac{4\pi}{5}\right)} = 6.76 V_I. \end{aligned} \tag{20}$$

Similarly, the output voltage amplitude is

$$V_m = \frac{1}{\pi}\int_0^{2\pi}\left(v_{DS3} - v_{DS1}\right)\sin\left(\omega t + \frac{9\pi}{10}\right) d\left(\omega t\right) = \frac{4V_I}{\pi}. \tag{21}$$

Applying Ohm's Law, $V_{Lm} = I_m \omega L_s$ and $V_m = I_m R_s$. Therefore, the ratio V_{Lm}/V_m is

$$\frac{V_{Lm}}{V_m} = \frac{\omega L_s}{R_s} = \frac{6.76 V_I}{\frac{4V_I}{\pi}} = 5.31. \tag{22}$$

Furthermore, the output power is given by

$$P_O = \frac{V_m^2}{2R_s} = \frac{\left[\frac{2}{\pi} V_I \left(1 - \cos\frac{4}{5}\pi\right)\right]^2}{2R_s}, \tag{23}$$

from which

$$R_s = \frac{V_m^2}{2P_O}. \tag{24}$$

The input power of the inverter is $P_I = V_I I_m$. Using (12)

$$\begin{aligned} P_I = V_I I_m &= \frac{\omega V_I^2}{\pi} \frac{1 - \cos\frac{4}{5}\pi}{1 + \cos\frac{4}{5}\pi} \left(C_{sw1} + C_{sw4}\right) \\ &= 3.01 \omega V_I^2 (C_{sw1} + C_{sw4}). \end{aligned} \tag{25}$$

B. Circuit Components

Assuming the inverter efficiency as unity, the $P_O = P_I$. If the shunt capacitances are equal to C_{sw}, then combining (11) and (25) provides

$$C_{sw} = \frac{\pi P_O}{\omega V_I^2} \frac{1 + \cos\frac{4}{5}\pi}{1 - \cos\frac{4}{5}\pi} = 0.33 \frac{P_O}{\omega V_I^2}. \tag{26}$$

The quality factor of the series resonant tank responsible to provide a pure sinusoidal current waveform is

$$Q_s = \frac{\omega_s \left(L_a + L_s\right)}{R_s} = \frac{\omega_s L}{R_s}. \tag{27}$$

Modifying (27), the inductance L_a is

$$L_a = L - L_s = \left(Q_s - \frac{V_{Lm}}{V_m}\right) \frac{R_s}{\omega_s}, \tag{28}$$

where V_{Lm}/V_m is as given in (22). The components L_a and C_r are tuned to resonate at the switching frequency f_s. Therefore,

$$\omega_s = \frac{1}{\sqrt{L_a C_r}} = 2\pi f_s. \tag{29}$$

The resonant capacitance is expressed as

$$C_r = \frac{1}{\omega_s^2 L_a} = \frac{1}{\omega_s R_s \left(Q_s - \frac{V_{Lm}}{V_m}\right)}. \tag{30}$$

Since $L = L_a + L_s$, the the resonant frequency between C_r and L is

$$\omega_p = \frac{1}{\sqrt{LC_r}}. \tag{31}$$

The inductance L_s in the series form can be converted into L_m in parallel to the load inductance. In the version of the inverter as shown in Fig. 1(a), L_m represents the magnetizing inductance of transformer. Let the loaded quality factor be

$$q_l = \frac{\omega_s L_s}{R_s}. \tag{32}$$

Converting the series $L_s - R_s$ combination to a parallel $L_m - R_p$ network has been described in [12]. Thus, the parallel inductance L_m and the resistance R_p are

$$L_m = L_s \left(1 + \frac{1}{q_l^2}\right). \tag{33}$$

$$R_p = R_s \left(1 + q_{load}^2\right). \tag{34}$$

IV. Voltage Transfer Function and Efficiency

A. Voltage Transfer Function

From the waveforms in Fig. 2, the tank voltage at the input of the resonant tank

$$v_{tan} = \frac{-2I_m}{\omega(C_{sw2} + C_{sw3})} \left[\sin\left(\omega t + \frac{4\pi}{10}\right) + \cos\left(\frac{\pi}{5}\right)\right] + V_I, \tag{35}$$

for the intervals $0 \le \omega t < \frac{3}{10}\pi$ and $\frac{17}{10}\pi \le \omega t < \frac{23}{10}\pi$. During the intervals $\frac{3}{10}\pi \le \omega t < \frac{7}{10}\pi$ and $\frac{13}{10}\pi \le \omega t < \frac{17}{10}\pi$, the value of the tank voltage is V_I. Similarly, during $\frac{7}{10}\pi \le \omega t < \frac{13}{10}\pi$

$$v_{tan} = \frac{2I_m}{\omega(C_{sw2} + C_{sw3})} \left[\sin\left(\omega t + \frac{4\pi}{10}\right) - \cos\left(\frac{\pi}{5}\right)\right] + V_I \tag{36}$$

Combining these voltages, the fundamental component is

$$\begin{aligned} v_{tan1} &= V_{tan1m} \sin\left(\omega t - \theta\right) \\ &= V_{Lm} \cos\left(\omega t - \frac{3}{5}\pi\right) + V_m \sin\left(\omega t - \frac{3}{5}\pi\right), \end{aligned} \tag{37}$$

where

$$V_{tan1m} = \sqrt{V_{Lm}^2 + V_m^2}, \quad \text{and} \quad \theta = \phi + \psi. \tag{38}$$

In (38), θ is the phase of the fundamental tank voltage, $\phi = -\pi/10$ as obtained in (8), and ψ is the phase shift introduced by the resonant tank. The rms value of the fundamental tank voltage is $V_{tan1rms} = V_{tan1m}/\sqrt{2}$. The voltage transfer function of the full-bridge Class-DE inverter is

$$M_{VS} = \frac{V_{tan1rms}}{V_I}, \tag{39}$$

and the voltage transfer function of the resonant circuit is

$$M_{VR} = \frac{v_o}{V_{tan1rms}} = |M_{vr}| \, e^{j\alpha}. \tag{40}$$

Thus, the overall voltage transfer function of the inverter is

$$\begin{aligned} M_{VI} = M_{VS} M_{VR} &= \frac{v_o}{V_I} \\ &= \frac{\sqrt{V_{Lm}^2 + V_m^2}}{\sqrt{2} V_I} |M_{vr}| \, e^{j\alpha}. \end{aligned} \tag{41}$$

In (41), the magnitude $|M_{vr}|$ and phase α are

$$|M_{VR}| = \frac{1}{\sqrt{(1+A)^2[1 - f_n^2]^2 + \frac{1}{Q_L^2}\left(\frac{1}{f_n}\frac{A}{A+1} - f_n\right)^4}} \tag{42}$$

$$\alpha = \tan^{-1}\left[\frac{1}{Q_L}\frac{\left(\frac{1}{f_n}\frac{A}{A+1} - f_n\right)^2}{(1+A)(1-f_n^2)}\right], \tag{43}$$

respectively. The ratio of the resonant to magnetizing inductance is

$$A = \frac{L}{L_m}. \tag{44}$$

The ratio of the series-parallel resonant frequency to the switching frequency is the normalized frequency given by

$$f_n = \frac{f_p}{f_s}. \tag{45}$$

The quality factor of the series-parallel tank is

$$Q_p = \omega_p C_r R_p = \frac{R_p}{\omega_p (L_r + L_m)}. \tag{46}$$

B. Input Impedance

The characteristic impedance of the resonant circuit is

$$Z_o = \sqrt{\frac{L_r + L_m}{C}}. \tag{47}$$

The input impedance of the series-parallel tank is

$$Z_i = R_p \frac{(1+A)\left(1-f_n^2\right) + j\frac{1}{Q_P}\left(\frac{1}{f_n}\frac{A}{1+A} - f_n\right)}{1 - jQ_P f_n (1+A)}. \tag{48}$$

Thus, the ratio of the magnitude of the input impedance to the characteristic impedance is

$$\frac{|Z_i|}{Z_O} = Q_p \sqrt{\frac{(1+A)^2(1-f_n^2)^2 + \frac{1}{Q_P^2}\left(\frac{1}{f_n}\frac{A}{1+A} - f_n\right)^2}{1 + \left[Q_P f_n (1+A)\right]^2}}. \tag{49}$$

Using (38) and (49), the amplitude of the current through the resonant tank is

$$I_{tan1m} = \frac{V_{tan1m}}{|Z_i|} = \frac{V_{Lm}^2 + V_m^2}{|Z_i|}. \tag{50}$$

C. Efficiency

The overall power loss in the resonant circuit is [12]

$$\begin{aligned} P_{loss} &= P_{Cr} + P_{Lr} + P_{DS} + P_{Csw} \\ &= (r_{Cr} + r_{Lr}) I_{tan1rms}^2 + 4 r_{DS} I_{DSrms}^2 \\ &\quad + 8 r_{Csw} I_{Cswrms}^2, \end{aligned} \tag{51}$$

where the rms value of the tank current is

$$I_{tan1rms} = \frac{I_{tan1m}}{\sqrt{2}}, \tag{52}$$

the rms value of the MOSFET current is

$$I_{DSrms} = \frac{I_{tan1m}}{2}\sqrt{\frac{1}{2\pi}\left[\frac{8}{5}\pi - \sin\left(\frac{8}{5}\pi\right)\right]} = 0.487 I_{tan1m}, \tag{53}$$

the rms value of the current through the shunt capacitance is

$$I_{Cswrms} = \frac{I_{tan1m}}{2}\sqrt{\frac{1}{8\pi}\left[\frac{2}{5}\pi + \sin\left(\frac{8}{5}\pi\right)\right]} = 0.055 I_{tan1m}. \tag{54}$$

The rms value of the current through the load resistance is

$$I_{Rprms} = \frac{1}{R_p}\sqrt{\frac{V_{Lm}^2 + V_m^2}{2}}\,|M_{vr}|\,. \tag{55}$$

Therefore, the inverter output power is

$$P_{Rp} = I_{Rprms}^2 R_p = \frac{V_{Lm}^2 + V_m^2}{2R_p} M_{vr}^2. \tag{56}$$

Finally, the inverter efficiency can be determined as

$$\eta_I = \frac{1}{1 + \frac{P_{Rp}}{P_{loss}}}. \tag{57}$$

V. Class-DE Inverter Simulation Results

A. Design Example

An inverter with design specification as follows is designed: DC input voltage $V_I = 230$ V, output power $P_O = 921$ W, and switching frequency $f_s = 100$ kHz. A duty cycle $D = 0.4$ is considered. The dead time is $t_d = 0.1$. Using (14), the values of the shunt capacitances are $C_{sw} = 4.25$ nF. Let us assume the quality factor $Q_s = 10$. From (12), $R_s = 37.2\Omega$, from (15), $L = 592$ μH, from (16) $L_a = 565.65$ μH to yield $L_s = 26.35$ μH, and from (17), $C_r = 4.48$ nF. For the series-parallel resonant circuit we have $L_m = 166.2$ μH and $R_p = 44.1\Omega$. The parasitic resistances of the MOSFET are $r_{DS} = 15$ mΩ, shunt and resonant capacitor $r_{Csw} = r_{Cr} = 0.656$ Ω, and resonant inductor $r_L = 0.110$ Ω. According to (31), the inverter voltage transfer function is $M_{VI} = 0.89$. Thus, the amplitude of the output voltage of the series-parallel network is $V_m = 204$ V. Furthermore, the overall inverter power loss was calculated as $P_{loss} = 23.3$ W. The inverter efficiency calculated using (57) was $\eta_I = 97.6\%$.

B. Simulation Results

The inverter designed in the previous section and shown in Fig. 1 was simulated on SABER circuit simulator. Fig. 3 shows the waveforms of the current and voltage waveforms of MOSFETs S_1 illustrating the ZVS operation. A small portion of the switch current flows through the anti-parallel diode, causing its drain-source voltage to be equal to zero. Fig. 4 shows the waveforms of the tank current i_{tan}, tank voltage v_{tan}, output voltage v_o, and output power p_{Rp}. The rms value of the output current and voltage were 4.98 A and 185 V, respectively. The measured rms output power was 921 W, the measured input power was 958 W. The measured overall efficiency was 96% confirming the theoretical analysis.

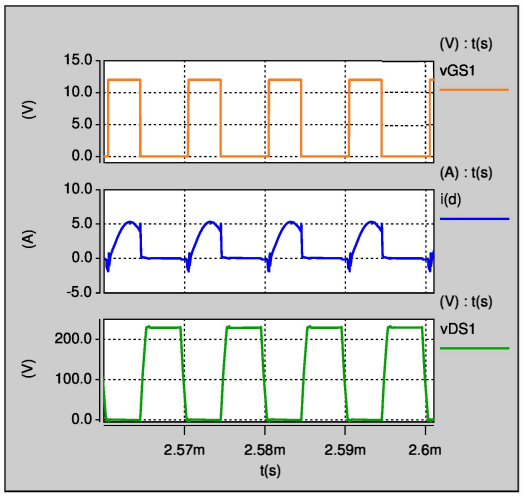

Fig. 3. Simulated waveforms of the gate-to-source voltage v_{GS1}, drain-to-source voltage v_{DS1}, and drain current i_{D1} of the MOSFET S_1 showing ZVS operation.

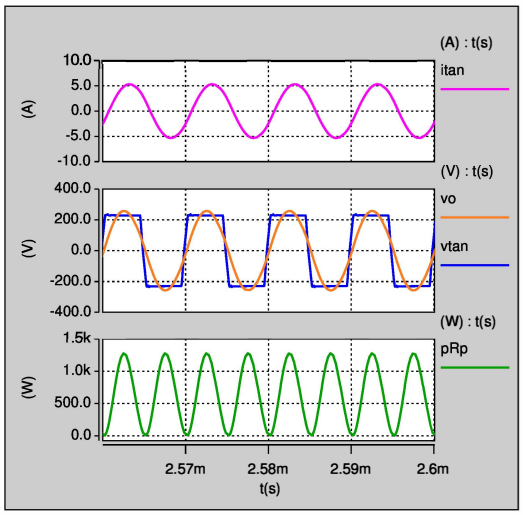

Fig. 4. Simulated waveforms of the tank current i_{tan}, tank voltage v_{tan}, output voltage v_o, and output power p_{Rp}.

VI. Conclusions

This paper has presented the following for a full-bridge Class-DE resonant inverter operating at a fixed duty ratio: (a) steady-state analysis using first-harmonic approximation and (b) derivation of closed-form expressions for the currents, voltages, and powers. The design procedure has been formulated for a series resonant tank circuit. Using transformation principles, the series resonant network has been transformed into a series-parallel resonant topology in order to accommodate the magnetizing inductance of the transformer. The expressions to calculate the values of resonant circuit component and the wave-shaping shunt capacitances of the inverter-bridge have been derived. The voltage transfer function and the input impedance of the series-parallel topology have been analyzed. The expression for the overall efficiency of the inverter has been derived. Simulations have been performed on an inverter operating at a supply voltage of 230 V, output power of 920 W, and at a switching frequency of 100 kHz. The simulation results show the validity of the theoretical predicted analysis.

References

[1] H. Sekiya, X. Wei, T. Nagashima, and M. K. Kazimierczuk, "Steady state analysis and design of class-DE inverter at any duty ratio," *IEEE Trans. Power Electron.*, vol. 30, no. 7, pp. 3685-3694, July 2015.

[2] H. Sekiya, N. Sagawa, and M. K. Kazimierczuk, "Analysis of class DE amplifier with nonlinear shunt capacitances at any grading coefficient for high Q and 25% duty ratio," *IEEE Trans. Power Electron.*, vol. 25, no. 4, pp. 924-932, Apr. 2010.

[3] M. Amjad, Z. Salam, M. Facta, and S. Mekhilef, "Analysis and implementation of transformerless LCL resonant power supply for ozone generation," *IEEE Trans. Power Electron.*, vol. 28, no. 2, pp. 650-660, Feb. 2013.

[4] H. Sarnago, O. Lucia, A. Mediano, and J. M. Burdio, "Class-D/DE dualmode-operation resonant converter for improved-efficiency domestic induction heating system," *IEEE Trans. Power Electron.*, vol. 28, no. 3, pp. 1274-1285, Mar. 2013.

[5] T. Suetsugu and M. K. Kazimierczuk, "Integration of class DE inverter for on-chip power supplies," *Proc. IEEE Intl. Symp. Circ. Syst.*, Island of Kos, Greece, May 2006, pp. 3133-3136.

[6] T. Suetsugu and M. K. Kazimierczuk, "Integration of class DE dc-dc converter for on-chip power supplies," *Proc. IEEE Power Electron. Specialist Conf.*, Jeju, South Korea, Jun. 2006, pp. 1-5.

[7] D. Murthy-Bellur, A. Bauer, W. Kerin, and M. K. Kazimierczuk, "Inverter using loosely coupled inductors for wireless power transfer," *Proc. IEEE Intl. Midwest Symp. Circ. Syst.*, Boise, ID, USA, Aug. 2012, pp.1164-1167.

[8] K. Inoue, T. Nagashima, X. Wei, and H. Sekiya, "Design of high-efficiency inductive-coupled wireless power transfer system with class-DE transmitter and class-E rectifier," *Proc. IEEE Industrial Electronics Society*, Vienna, Austria, Nov. 2013, pp. 613-618.

[9] M. K. Kazimierczuk, N. Thirunarayan, and S. Wang, "Analysis of series parallel resonant converter," *IEEE Trans. Aerosp. and Electron. Syst.*, vol. 29, no. 1, pp. 88-99, 1993.

[10] J. Modzelewski, "Optimum and sub-optimum operation of high-frequency Class-D zero-voltage-switching tuned power amplifier," *Bull. Polish Acad. Sci., Tech. Sci.*, vol. 46, no. 4, pp. 458-473, Apr. 1998.

[11] M. K. Kazimierczuk and J. Jozwik, "Resonant dc/dc converter with class E inverter and class-E rectifier," *IEEE Trans. Ind. Electron.*, vol. 36, no. 4, pp. 468-478, Apr. 1989.

[12] M. K. Kazimierczuk, *RF Power Amplifiers*, 2nd Ed., John Wiley Sons, Chichester, UK, 2014.

[13] M. K. Kazimierczuk and D. Czarkowski, *Resonant Power Converters*, 2nd Ed., John Wiley Sons, Hoboken, NJ, 2012.

[14] M. Hayati, A. Lotfi, M. K. Kazimierczuk, and H. Sekiya, "Analysis and design of class-E power amplifier with MOSFET parasitic linear and nonlinear capacitances at any duty ratio," *IEEE Trans. Power Electron.*, vol. 28, no. 11, pp. 5222-5232, Nov. 2013.

[15] A. Mediano and P. Molina, "Frequency limitation of a high-efficiency class E tuned RF power amplifier due to a shunt capacitance," *Proc. IEEE MTT-S Intl. Microwave. Symp. Dig.*, Anaheim, CA, USA, Jun. 1999, pp. 13-19.

[16] A. Mediano, P. Molina, and J. Navarro, "Class E RF/microwave power amplifier: Linear Equivalent of transistors nonlinear output capacitance, normalized design and maximum operating frequency versus output capacitance," *Proc. IEEE MTT-S Int. Microw. Symp. Dig.*, Boston, MA, USA, Jun., 2000, pp. 783-786.

[17] X. Wei, H. Sekiya, S. Kuroiwa, T. Suetsugu, and M. K. Kazimierczuk, "Design of class-E amplifier with MOSFET linear gate-to-drain and nonlinear drain-to-source capacitances," *IEEE Trans. Circuits Syst.-I*, vol. 58, no. 10, pp. 2556-2565, Oct. 2011.

[18] T. Suetsugu and M. K. Kazimierczuk, "Maximum operating frequency of class-E amplifier at any duty ratio," *IEEE Trans. Circ. Syst.-II,* vol. 55, no. 8, pp. 768-770, Aug. 2008.

[19] M. K. Kazimierczuk and W. Szaraniec, "Class D zero-voltage switching inverter with only one shunt capacitor," *IEE Proceedings, Part B, Electric Power Appl.*, vol. 139, pp. 449-456, Sept. 1999.

[20] A. Ayachit, D. K. Saini, T. Suetsugu, and M. K. Kazimierczuk, "Three-coil wireless power transfer system using Class-E2 resonant dc-dc converter," *Proc. IEEE Intl. Telecommunications Energy Conf., INTELEC*, Yokohama, Japan, October 2015, pp. 1116-1119.